



## ORIGINAL ARTICLE

# Formulation of gold nanoparticles with hibiscus and curcumin extracts induced anti-cancer activity



Sultan Akhtar <sup>a,\*</sup>, S.M. Asiri <sup>a</sup>, Firdos Alam Khan <sup>b</sup>, S.T. Gunday <sup>a</sup>, Arfa Iqbal <sup>c</sup>,  
Noor Alrushaid <sup>b</sup>, O.A. Labib <sup>d</sup>, G.R. Deen <sup>e</sup>, F.Z. Henari <sup>e,\*</sup>

<sup>a</sup> Department of Biophysics, Institute for Research & Medical Consultations, Imam Abdulrahman Bin Faisal University, Post Box No. 1982, Dammam 31441, Saudi Arabia

<sup>b</sup> Department of Stem Cell Research, Institute for Research & Medical Consultations, Imam Abdulrahman Bin Faisal University, Post Box No. 1982, Dammam 31441, Saudi Arabia

<sup>c</sup> Institute of Environmental Engineering and Research, University of Engineering and Technology, Lahore 54890, Pakistan

<sup>d</sup> Department of Environmental Health, College of Public Health, Imam AbdulRahman Bin Faisal University, P.O. Box 1982, Dammam 31441, Saudi Arabia

<sup>e</sup> Department of Biosciences, School of Medicine, Royal College of Surgeons in Ireland (RCSI), Medical University of Bahrain, Bahrain

Received 30 September 2021; revised 23 November 2021; accepted 24 November 2021

Available online 27 November 2021

## KEYWORDS

Gold nanoparticles;  
Green synthesis;  
Hibiscus;  
Curcumin;  
Anticancer

**Abstract** Gold nanoparticles (AuNPs) have shown a potential for biological applications due to their biocompatibility and high efficiency in drug delivery. Most of the times, the chemical routes are being used to synthesize the AuNPs products. In this paper, eco-friendly non-chemical route was used to prepare AuNPs by utilizing hibiscus and curcumin extracts as reducing and stabilizing agents, and subsequently their anticancer activities were investigated. The synthesized AuNPs were characterized by using ultraviolet–visible spectroscopy (UV–Vis spectroscopy), Fourier transform infrared (FTIR) spectroscopy, scanning electron microscopy (SEM), and transmission electron microscopy (TEM). UV–Vis spectroscopy analysis confirmed the characteristic absorption peak of gold, and FTIR findings were highlighted the characteristic bonding. SEM and TEM analyses showed that the particles were predominantly spherical in shape. The particles were well dispersed when they were prepared under Hibiscus extracts with average size ~ 13 nm. An interesting morphology was observed when AuNPs were prepared with curcumin, where particles displayed an interconnected morphology (average size ~ 18 nm). The anticancer cell activity of AuNPs was studied against human colorectal carcinoma cells (HCT-116) and breast cancer cells (Michigan Cancer

\* Corresponding authors.

E-mail addresses: [suakhtar@iau.edu.sa](mailto:suakhtar@iau.edu.sa) (S. Akhtar), [fzhenari@rcsi-mub.com](mailto:fzhenari@rcsi-mub.com) (F.Z. Henari).

Peer review under responsibility of King Saud University.



Foundation-7 (MCF-7)). The results of anticancer study showed that the treatment of cancer cells with AuNPs decreased the number of cells significantly as compared to control cells. The AuNPs - Hibiscus specimen showed a better inhibiting property than AuNPs -Curcumin, which is attributed to their uniform dispersion and small size.

© 2021 The Authors. Published by Elsevier B.V. on behalf of King Saud University. This is an open access article under the CC BY-NC-ND license (<http://creativecommons.org/licenses/by-nc-nd/4.0/>).

## 1. Introduction

Nanotechnology deals with the design, innovation and production of nanoscale materials in the range of 1 to 100 nm (Lee, 2020). The nanomaterials with dimension between 1 and 100 nm can be conjugated and modified with biological systems depending on cell sort and targeted organelles by adopting diverse strategies and approaches. For instance, the modifications and functionalization of nanoparticles could be performed by utilizing their surface properties, structures, the molecule measure and state of accumulation (Zhang, 2015). Start from the discovery, different types of nanoparticles have been tested whereby the gold nanoparticles (AuNPs) have shown significant future promises and applications especially in the field of biological sciences due to their biocompatibility and high efficiency in drug delivery (Xu, 2021).

Recently, the extraordinary features of AuNPs have been studied and analyzed to discover their productive features for the development of biomedicine. The size, shape, structures, surface coating and surface-to-volume ratio are the most important properties of any types of nanoparticles which define the effectiveness of the nanoparticles during their interaction with other materials (Taghizadeh, 2019). The electronic structure of AuNPs offers a large number of opportunities to utilize them in clinical applications, specifically in radiotherapy and radiography applications (Zhang, 2015). AuNPs have gained a considerable attention in the field of nanomedicine owing high biocompatibility and high efficiency which subsequently expanded their applications to other fields such as, biomedical imaging, radiation dose enhancement, biosensor, detection of human pathogens, gene transfer, nucleic acid labelling, therapeutic agents, sensing agents, drug delivery, antibacterial activity, and as molecular therapeutics (Zhang, 2015; Vimalraj et al., 2018; AbuMousa, 2018; Jermy, 2021; Ansari, 2021; Jain et al., 2012; Peng and Liang, 2019).

Generally, two techniques are widely used for the preparation of nanoparticles, top-down and bottom-up. These preparation approaches could be categorized as chemical, physical and biological approaches (Elahi et al., 2018). Recent endeavors have been committed to use such synthesis routes which allows the researchers to control the physical parameters of the particles such as the morphology, structure, size, solubility, stability and functionality (Yeh et al., 2012). The conventional chemical routes such as sonochemical, sol-gel, hydrothermal, etc. were often use the toxic and hazardous chemicals for the preparation of AuNPs along with costly chemical processes. The constant use of such chemical routs could increase the environmental hazards and hence render their clinical applications despite having attractive properties (Vimalraj et al., 2018; Daruich De Souza et al., 2019). On the other hand, the biosynthesis methods have achieved a considerable attention of the researchers by employing either microorganisms (fungi,

bacteria, actinomycetes, yeast, etc.) or plant tissues (root, leaf, pectin, stem, seed, peel, fruit, flower, etc.) for the preparation of AuNPs. Green synthesis routs are more significant and interested due to their simplicity and ability to complete quickly during the preparation of nanomaterials (Ahmed, 2016). Amongst the alternative methods, the plant extracts are simpler for mass-production applications and proved to be eco-friendly, relatively cheaper and safe for human and its environment due to use of biodegradable organic agents (Zhao et al., 2013). From various plants, hibiscus has been implemented in oriental medicine to treat various diseases such as neuroprotective activity (Kim, 2018) anti-aging (Yang, 2019) antibacterial (Bindhu, 2014) anti-inflammation efficacy (Xu, 2021) and anti-cancer (Hsu, 2015). Hibiscus leaf extraction was utilized to synthesis several forms and morphologies of AuNPs where the particle average diameter was achieved as small as 13 nm (Ahmed, 2016). Also, curcumin has been utilized as a green synthesise approach for the preparation of AuNPs where curcumin extraction was acting as reducing and stabilizing agent at room temperature (Al Shehab and Patra, 2021). Importantly, by varying the loading of curcumin and its derivatives, the size, shape and the dispersity of the AuNPs can be controlled and tailored (Muniyappan et al., 2021).

The plant extracted AuNPs have been investigated in the area of medicine, such as utilized as an antioxidant, antibacterial agents, antimicrobial and anticancer proliferations (Wang, 2019). Due to their significant quenching efficiencies, surface modifiability and biocompatibility, AuNPs have become exceedingly doable materials for tumor treatment and for the purpose of inventive systems for cancer therapy (Farooq, 2018). In addition, AuNPs could be used for diagnostics (theragnostic) and combined therapy, such as radiation sensitizers, photo thermal ablation of tumors and real time imaging, owing to their multifunctional properties (Yeh et al., 2012).

The size, distribution and surface modification of AuNPs could greatly affect their physical and chemical properties such as antibacterial properties in that study (Gu, 2020). With respect to surface modification; different kinds of molecules can be associated with AuNPs during preparation to create special biological activities (Liu and Lämmerhofer, 2019). In this study, AuNPs are synthesized using hibiscus and curcumin extractions, and evaluate their anticancer activities against: (1) human colorectal carcinoma (HCT-116) and (2) human breast adenocarcinoma cells (known as Michigan Cancer Foundation-7 (MCF-7)). The reason for choosing curcumin and hibiscus extractions is that they have been used traditionally in the medical field for different types of diseases. The plant extractions are usually contained sugars, terpenoids, polyphenols, alkaloids, phenolic acids, and protein. These phytochemicals are responsible for reducing and stabilizing the metal nanoparticles (Shahwan, 2011). The chemical bindings,

optical properties, and morphological features of the prepared AuNPs are characterized using ultraviolet–visible (UV–Vis) spectroscopy), Fourier transform infrared (FTIR) spectroscopy, scanning electron microscopy equipped with energy dispersive X-rays spectroscopy (SEM/EDS), and transmission electron microscopy (TEM) with selected electron diffraction (TEM/SAED) techniques. The anticancer capabilities of the prepared AuNPs (AuNPs-hibiscus and AuNPs-curcumin) are tested against HCT-116 and MCF-7 cells using morphometric and bioassay. The important morphological features of the treated and untreated cells are examined under inverted microscope and calculate their cell viability.

## 2. Experimental details

### 2.1. Synthesis of AuNPs-Hibiscus and AuNPs-Curcumin

Sample 1 (AuNPs-Hibiscus specimen): *Hibiscus rosa sinensis* flowers were collected from the trees on the campus, washed several times, and rinsed with distilled water to remove dust particles. The washed flowers were dried in an oven at a temperature of 60 °C for 24 h. The dried flowers were ground with a blender for making the fine powder. Five grams of fine powder was added in 100 ml water. Double-distilled water was used throughout the experiments for the synthesis of AuNPs. The powder/water mixture was then boiled, stirred for 10 min, and filtered twice using filter paper (Whatman filter paper No.1). Now, 0.4 g of chloroauric salt ( $\text{HAuCl}_4 \cdot 3\text{H}_2\text{O}$ ) was dissolved in 100 ml of water in order to prepare 10 mM of  $\text{HAuCl}_4 \cdot 3\text{H}_2\text{O}$  solution. The prepared extraction was diluted four times, 100 ml from the diluted extract was placed in an Erlenmeyer flask and added 120 ml gold salt solution into it. The extract/gold salt mixture was heated in a microwave oven of 1000 W for 20 sec. The immediate color change of the solution from light yellow to purple was observed after microwave heating. The color change is an indication for the

formation of AuNPs. The pictorial representation of the preparation of AuNPs using Hibiscus extraction, referred as AuNPs -Hibiscus (sample 1) is depicted along with digital photo of extraction and prepared AuNPs in Fig. 1a & a1.

Sample 2 (AuNPs-Curcumin): The turmeric extract was prepared by adding 25 mg of dried powder bought from a local supermarket to 100 ml of water and vortexed for 5 min. The turmeric powder was chosen because more phytochemicals responsible for reduction are present relative to purified curcumin. The solution was left undisturbed for 10 minutes to allow undissolved turmeric to precipitate and then filtered in a similar way as described above for sample 1. To prepare a 10 mM of  $\text{HAuCl}_4 \cdot 3\text{H}_2\text{O}$  solution, 0.395 g of  $\text{HAuCl}_4 \cdot 3\text{H}_2\text{O}$  was dissolved in 100 ml of water and vortexed for 3 min at a medium speed. To synthesize the gold nanoparticles (AuNPs), 10 ml of the 10 mM  $\text{HAuCl}_4 \cdot 3\text{H}_2\text{O}$  solution was added to 0.5 ml turmeric solution in a clean sterilized Erlenmeyer flask. The solution was then heated for 20 s in a microwave oven of 1000 W. An alteration (change) in the color was observed, and the solution became dark purple. The color change in an indication of the reduction reaction which confirmed the formation of AuNPs. The pictorial representation of AuNPs preparation using Curcumin extract, the specimen referred to as AuNPs -Hibiscus (sample 2) is depicted by Fig. 1b & b1 along with digital photo of the extraction and prepared AuNPs. Further characterizations of the prepared AuNPs-hibiscus and AuNPs-curcumin specimens are carried out using widely used tools, such as SEM/EDS, TEM/SAED, FTIR and UV–Vis spectrometry before performing the anticancer experiments.

### 2.2. SEM and TEM characterization

The morphology and the structure of the colloidal nanoparticles (AuNPs -Hibiscus and AuNPs -Curcumin) was evaluated using scanning electron microscopy (SEM) (Model: Inspect

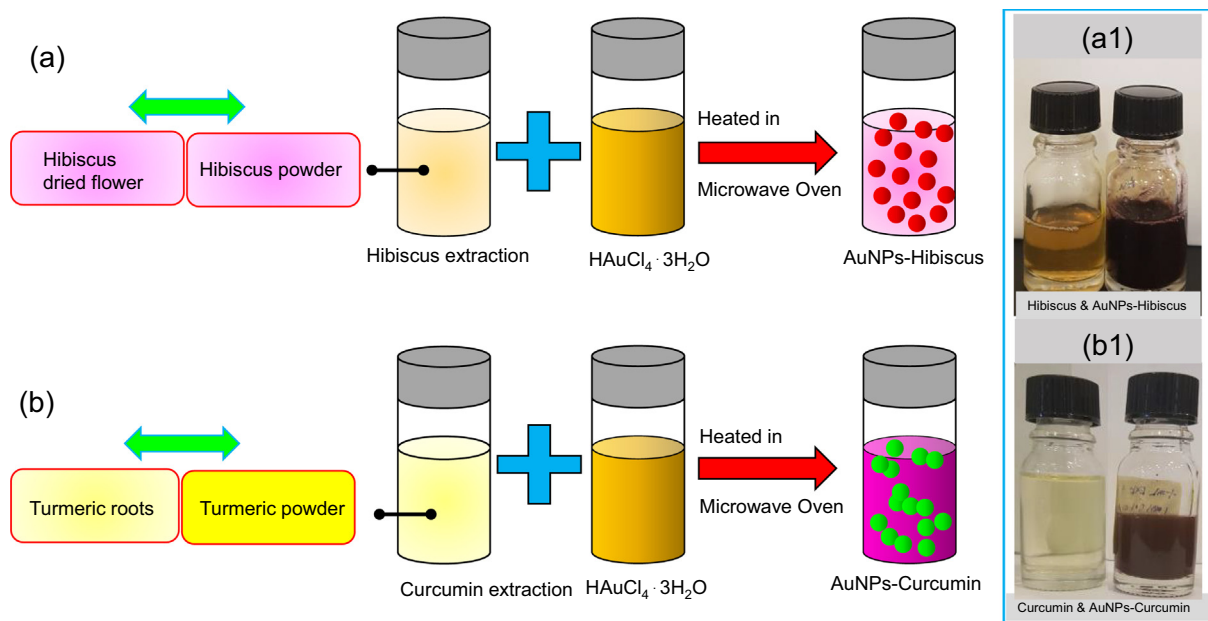


**Fig. 1** Schematic illustration of AuNPs preparation; (a) AuNPs-Hibiscus and (b) AuNPs-Curcumin along with digital photos of extractions and prepared AuNPs (a1, b2).

S50, FEI, at 20 kV). For SEM samples, the colloidal nanoparticles of each sample were dropped onto the SEM metal stubs covered with conducting doubled sided tape. The prepared stubs were air-dried and transport into the SEM chamber for examination. The SEM micrographs were taken at two magnifications, namely x50, 000 and x100, 000. Transmission electron microscopy (TEM) (Model: Morgagni 268, FEI, at 80 kV) was used at 80 kV in bright-field imaging mode for detailed morphology and structure of the prepared AuNPs. The size histograms were drawn by utilizing the particles as measured their sizes from the TEM images. The crystalline structure of the AuNPs -Hibiscus and AuNPs -Curcumin specimens were investigated by SAED patterns (selected area electron diffraction pattern), which were taken in the TEM. The detailed description of SEM and TEM methods is given elsewhere (Akhtar, 2020; Khan, 2020; Alheshibri, 2021).

### 2.3. UV-Vis and FTIR spectroscopy characterization

The optical properties of AuNPs-Hibiscus and AuNPs -Curcumin specimens were studied using ultraviolet-visible (UV-Vis) spectroscopy (Double-beam Shimadzu UV-1800 spectrophotometer). The absorption spectra of the specimens were taken between 350 and 800 nm with 1 nm resolution. The functional groups of the absorption bands of the specimens (AuNPs -Hibiscus and AuNPs -Curcumin) prepared using Hibiscus and curcumin were studied by Fourier transform infrared spectroscopy (FTIR: Nicolet 6700 with FTIR spectrometer, spectral range 400 – 4000  $\text{cm}^{-1}$ ) (Akhtar, 2018). For data analysis and explanation, the characteristics bands of each spectrum were labelled and highlighted between 4000 and 400  $\text{cm}^{-1}$ .

### 2.4. Anticancer characterization

#### 2.4.1. Treatment of AuNPs -Hibiscus and AuNPs -Curcumin

Two cancer cell lines: HCT-116 (human colorectal carcinoma) and MCF-7 (human breast adenocarcinoma cells) were purchased from American Type Culture Collection, United States of America (ATCC, USA) to study the impact of AuNPs on the cell viability. The cells of both the cell lines were cultured by applying the method as reported in our previous reports (Alheshibri, 2021; Akhtar, 2018; Mishra, 2016). In this method, the cells were cultured in the cultured media using 96-well plates in a  $\text{CO}_2$  incubator. 20,000 cells/well were seeded in the 96 cell culture plates. The chemicals in the cultured media are mentioned in our previous experiments. The grown cells were then treated with prepared products; AuNPs -Hibiscus and AuNPs -Curcumin for 48 h. In the control group, AuNPs -Hibiscus and AuNPs -Curcumin were not added. To examine the specificity of the AuNPs -Hibiscus and AuNPs -Curcumin specimens, non-cancer human cell line such as, HEK-293 (embryonic kidney cells) were also included in our studies.

#### 2.4.2. MTT assay

After 48 h, the cells were processed for the MTT assay as per previous studies (Gu, 2020; Liu and Lämmerhofer, 2019; Shahwan, 2011; Akhtar, 2020). The control groups, AuNPs -Hibiscus and AuNPs -Curcumin -treated groups were treated with 20  $\mu\text{l}$  of MTT, and treated cells were then further incu-

bated. After 4 h incubation in  $\text{CO}_2$  incubator, the cell culture media was changed with 1% of DMSO. The cell-well plates of both treated cells, HCT-116 and MCF-7 were analysed under ELISA plate reader (Model: Biotech Instruments, United States of America). Thereafter, the cell viability was found out for the statistical analysis using the following simple relation (1).

$$\text{Cell viability (in\%)} = \left[ \frac{(\text{optical density})_{\text{AuNPs-treated cells}}}{(\text{optical density})_{\text{untreated cells}}} \right] \times 100 \quad (1)$$

#### 2.4.3. Cancer DNA staining

DNA of the cancer cells was studied using DAPI (4',6-diamidino-2-phenylindole) staining assay (Liu and Lämmerhofer, 2019; Shahwan, 2011; Akhtar, 2020). DAPI is a fluorescent stain that binds strongly to A-T-rich regions in DNA. DAPI and PI only inefficiently pass through an intact cell membrane and therefore, preferentially stain dead cells. DAPI is a blue-fluorescent DNA stain that exhibits  $\sim 20$ -fold enhancement of fluorescence upon binding to AT regions of dsDNA. Because of its high affinity for DNA, it is also frequently used for counting cells, measuring apoptosis, sorting cells based on DNA content, and as a nuclear segmentation tool in high-content imaging analysis. In this assay, the grown cells were distributed into two groups: In the control group, where treatment of cells was not done with any nanoparticles. In the experimental group, cells were treated with AuNPs -Hibiscus (0.8  $\mu\text{g}/\text{ml}$ ) and AuNPs -Curcumin (0.8  $\mu\text{g}/\text{ml}$ ) in two separate batches. After 48-hour treatment, both groups (treated and untreated) were placed in the ice-cold paraformaldehyde environment and then with Triton X-100 in phosphate buffered saline (PBS). Thereafter, the cells were stained with DAPI staining chemicals for 5 min under a no-light environment. The cells were finally washed with PBS and cover slipped. In order to find the effect of the nanoparticles on the cancerous cells, the morphology of the treated and untreated cells was visualized under confocal scanning microscope (Model, Zeiss, Germany) after DAPI staining.

#### 2.4.4. Statistical analysis

The obtained data was displayed using mean ( $\pm$ ), standard deviation (SD) from triplicate experiments. The statistical data was obtained by using the one-way ANOVA and Dennett's post hoc test for statistical discussion.

## 3. Results and discussion

### 3.1. Physical, optical, and chemical analyses

The AuNPs were prepared using green synthesis method where hibiscus and curcumin extractions were utilized for reducing and stabilizing agents. During synthesis, the either prepared extraction (hibiscus or curcumin) was added to gold salt solution ( $\text{HAuCl}_4 \cdot 3\text{H}_2\text{O}$ ) and heated in a microwave oven. The formation of the colloidal AuNPs was judged by color change within the solution which changed immediately from light yellow to purple for AuNPs-Hibiscus and AuNPs-Curcumin from light orange to dark purple after microwave heating, see Fig. 2 (insets). The growth of AuNPs was further verified

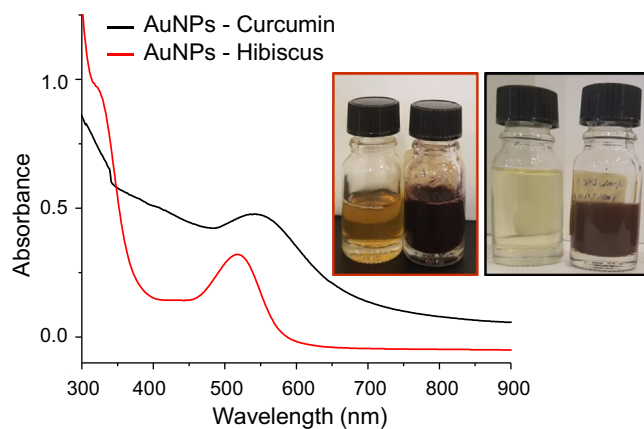


**Fig. 2** UV-Vis spectroscopy of AuNPs-Hibiscus (red spectrum) and AuNPs-Curcumin (black spectrum). Insets are digital photos of hibiscus extraction and prepared AuNPs (left), and curcumin extraction and prepared AuNPs (right).

by conducting the UV-Vis spectroscopy and analyzing the surface plasmon resonance (SPR) peak for both the prepared solutions, AuNPs -Hibiscus and AuNPs -Curcumin. Fig. 2 displays the UV-Vis spectroscopy results of the aqueous dispersion of AuNPs-hibiscus and AuNPs-curcumin. For AuNPs -Hibiscus, the spectra illustrate a sharp SPR peak at  $\sim 520$  nm, while a strong but relatively a broad peak at  $\sim 546$  nm for AuNPs - Curcumin (Mishra, 2016; Sreelakshmi, 2013; Muniyappan and Nagarajan, 2014). The SPR peak of AuNPs arises due to the oscillation of surface electrons in the conduction band of AuNPs in resonance with the incident wavelength. The appearance of a single absorption

peak suggested that the colloidal AuNPs are nearly spherical (Sun and Xia, 2003; Slocik, 2008). The position and width of the SPR absorption peak depend on the size and agglomeration of the gold NPs. The AuNPs synthesized with curcumin shows a broad absorption width with a redshift (about 15 nm) compared to nanoparticles synthesized with Hibiscus extraction which shows the sharp and narrower SPR peak. The redshift of SPR is due to the size (crystallites) increase of the gold nanoparticles as confirmed by TEM as shown below (SEM and TEM section).

FTIR spectroscopy technique is very useful for the identification of chemical bonding of the organic materials when conjugated with metallic nanoparticles. In this study, FTIR spectroscopy was carried out to study the active functional groups available in AuNPs when prepared with either using hibiscus or curcumin, the results of FTIR are shown in Fig. 3. The broad bands at about  $3203$  and  $3314$   $\text{cm}^{-1}$  are due to O-H stretching bond, for AuNPs -Hibiscus and AuNPs -Curcumin, respectively (Ismail, 2018). The peaks observed at approximately  $2920$  and  $2850$   $\text{cm}^{-1}$  are due to the C-H stretching mode (Bhuyan, et al., 2017). In the spectrum of AuNPs-Hibiscus, the weak band at  $1736$   $\text{cm}^{-1}$  is observed for the C = O stretching mode indicates the presence of carboxylic acid group (-COOH) of malic acid in the material bound to Au nanoparticles. However, for AuNPs-Curcumin, this band is very weak or rather absent. Moreover, the medium intense band at  $1344$   $\text{cm}^{-1}$  was appeared due to presence of C-O stretching mode. For AuNPs -Hibiscus, the amide II band at  $1646$   $\text{cm}^{-1}$  has become more prominent, while shifted to low wavenumber for AuNPs -Curcumin specimen (Philip, 2010). At  $1069$   $\text{cm}^{-1}$  and  $1018$   $\text{cm}^{-1}$ , the two additional peaks can be assigned to the C-O stretching frequency (Gurunathan, 2014). The intensity of the peaks reduced obviously for

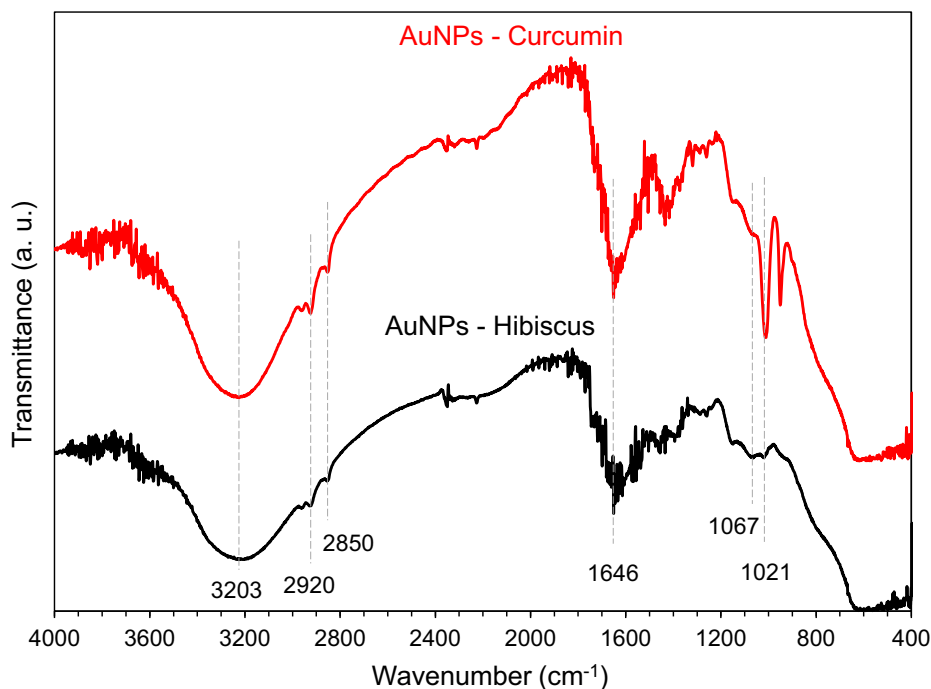


**Fig. 3** Fourier transform infrared (FTIR) spectra of AuNPs-Hibiscus and AuNPs- curcumin between  $4000$  and  $400$   $\text{cm}^{-1}$ . The characteristics bands are marked.

AuNPs-Curcumin and shifted to low wavenumber. It is obvious that proteins can attach to gold nanoparticles via free amine groups or carboxylate ions in amino acid residues (Ankamwar et al., 2005).

### 3.2. Morphological, elemental, and structural analyses

The physical, chemical, and biological properties of the prepared nanoparticles are greatly affected by the structure and the morphology. SEM and TEM are widely used tools to evaluate the size, shape, and structure of the nanoparticles at high resolution. The morphology and structure of the synthesized AuNPs-Hibiscus and AuNPs-Curcumin were analysed by SEM, EDS and TEM. Fig. 4 shows the SEM and EDS results of the gold nanoparticles of sample 1 (AuNPs-Hibiscus) and sample 2 (AuNPs-Curcumin). Sample 1 was prepared by adding of Hibiscus extraction into 10 mM of  $\text{HAuCl}_4 \cdot 3\text{H}_2\text{O}$  solution. A color change of the solution was observed upon heating the mixture into a microwave oven, an indication of the formation of gold nanoparticles. Similarly, sample 2 was prepared by using curcumin extraction and  $\text{HAuCl}_4 \cdot 3\text{H}_2\text{O}$  solution. Both the samples exhibited a compact morphology, confirming the presence of particles in the range of nanometers. The electronic images showed that the layer structure or sheet-like morphology composed of individual colloidal nanoparticles. However, the resolution of the SEM is limited to identifying the size, shape, and structure of the nanoparticles. Nevertheless, SEM revealed a large surface area of each

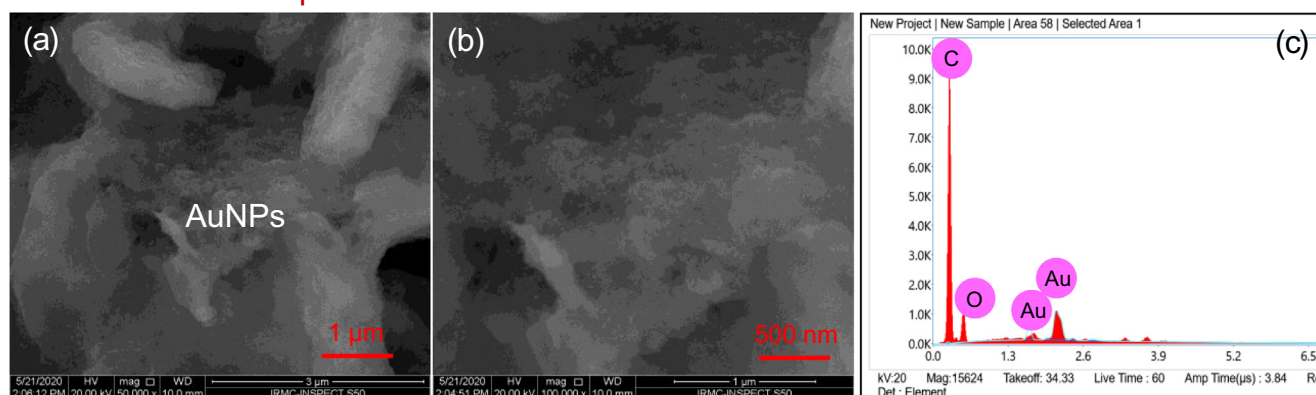
specimen, which is composed of AuNPs. EDS spectra showed the obvious peaks for the gold, near to 2.4 keV, confirming the successful preparation of AuNPs. Furthermore, TEM was carried out to reveal the size, shape, and structure of the colloidal specimens at high resolution. By TEM images as shown in Fig. 5, it can be seen that the particles displayed the perfect spherical shaped morphology. It was noted that particles were well dispersed on the support film in case of sample 1. In the case of sample 2, the particles were interconnected in the form of chain up to several nanoparticles. A slightly smaller size was found for specimen 1 as compared to specimen 2. The average particle size was estimated  $\sim 13$  and 18.3 nm, respectively (Fig. 5c & f). SAED analysis further confirms the nature of the particles, particles in both cases showed the crystalline structure as suggested by well-separated diffraction rings (signature of crystalline structure) with first four lattice planes were indexed as: (111), (200), (220) and (311), indicating face centered cubic (fcc) structure of gold (JCPDS: 04-0784) (Fig. 5b & e) (Sneha, 2010; Krishnamurthy, 2014). SEM/EDS and TEM/SAED analyses confirmed the formation of gold nanoparticles using Hibiscus and curcumin extractions.

### 3.3. Anticancer activities of AuNPs

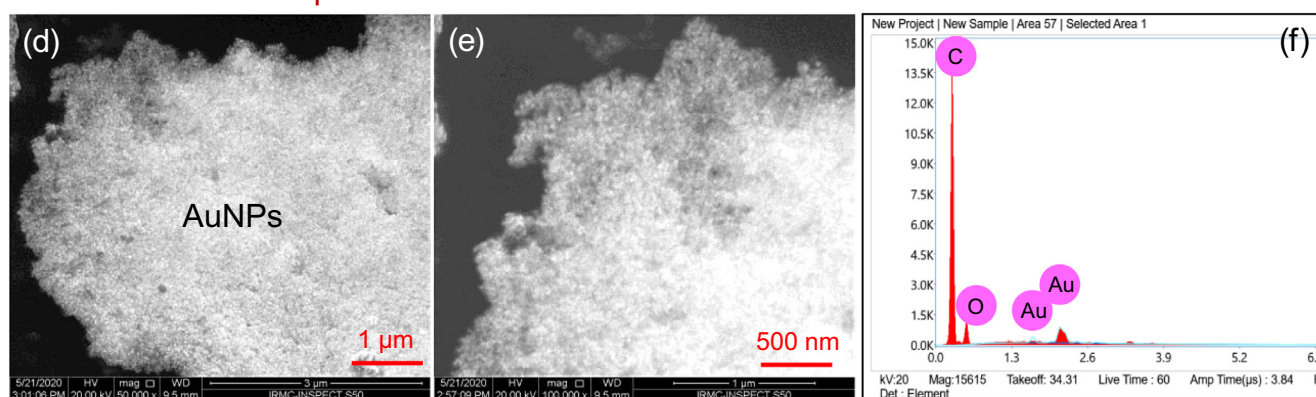
#### 3.3.1. Impact of AuNPs on cancer cells viability

The treatment of AuNPs -Hibiscus and AuNPs -Curcumin caused significant decreased in the number of cancer cells, as the number of DAPI stained cells were found to be signifi-

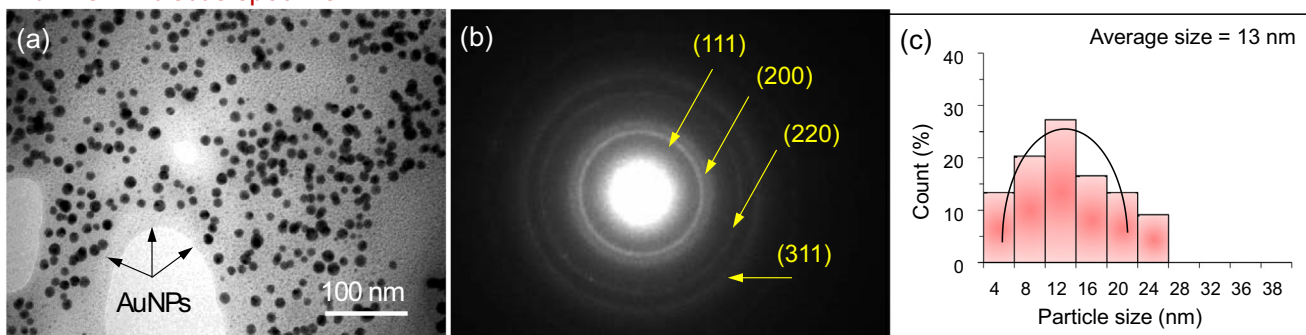
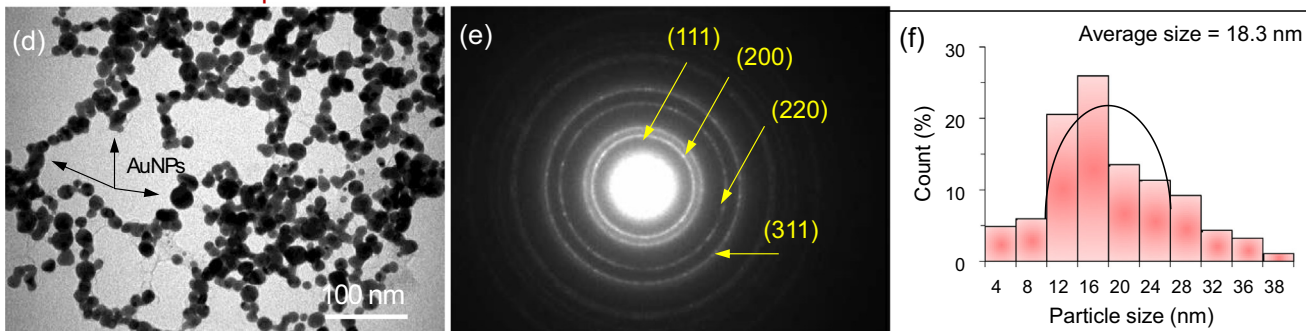
#### AuNPs - Hibiscus specimen



#### AuNPs - Curcumin specimen



**Fig. 4** SEM images of the prepared AuNPs-Hibiscus and AuNPs-Curcumin at two magnifications (x50, 000 and x100, 000) along with EDS spectra.

**AuNPs - Hibiscus specimen****AuNPs - Curcumin specimen**

**Fig. 5** TEM images, SAED patterns and size histograms of AuNPs. The AuNPs are marked with black arrows. The scale bars are 100 nm (a, d).

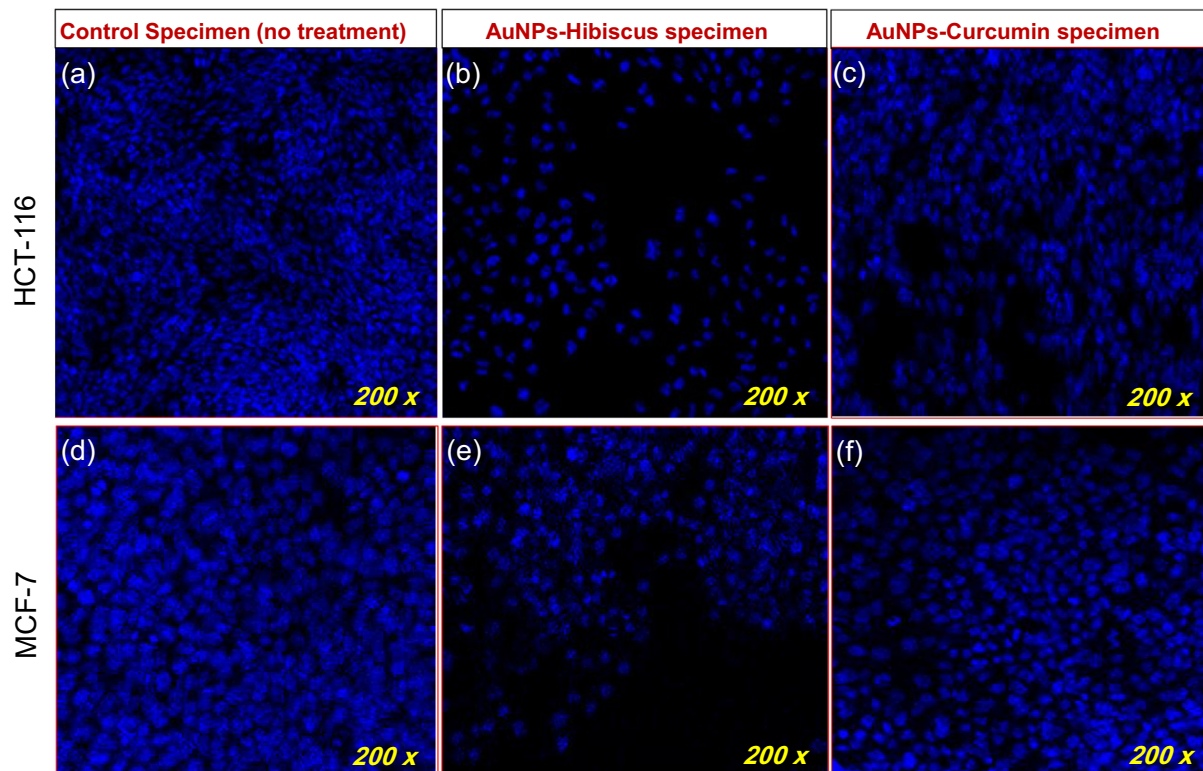


**Fig. 6** Disintegration of colon and breast cancer cell DNA (200x): (a-c) Impact of AuNPs-Hibiscus and AuNPs-Curcumin on colon cancer cells (HCT-116), post 48 h treatment (0.8  $\mu\text{g/ml}$ ). (d-f) Impact of AuNPs-Hibiscus and AuNPs-Curcumin on breast cancer cells (MCF-7) after treatment of 48 h (0.8  $\mu\text{g/ml}$ ).

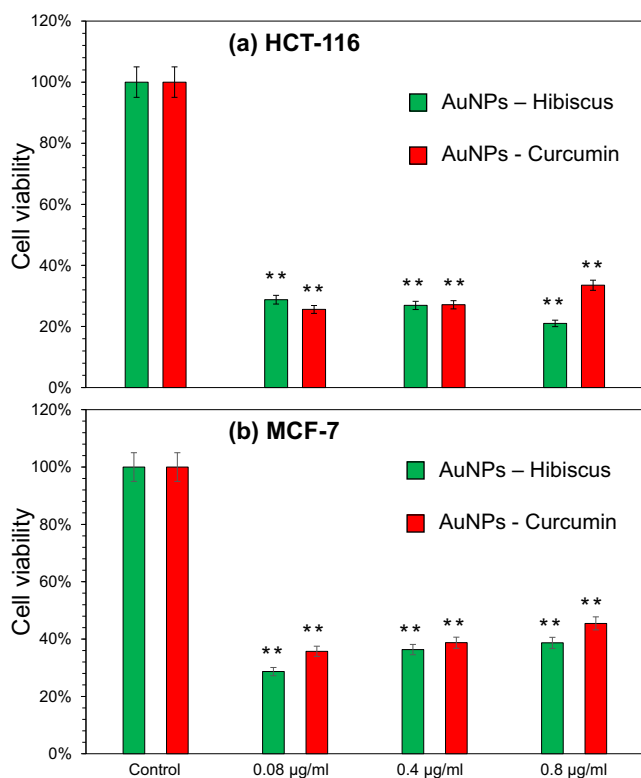


**Fig. 7** Cell viability assay: Impact of AuNPs-Hibiscus and AuNPs-Curcumin on (a) colon cancer cells (HCT-116) and (b) breast cancer cells (MCF-7). \*  $P < 0.05$ ; \*\*  $P < 0.01$ .

cantly less in the AuNPs -Hibiscus and AuNPs -Curcumin -treated cells as compared to control cells (Fig. 6). The decrease in the cancer cells for the treated specimens is due to the cell death due to systematic cell death (loss of life), also known as apoptosis. Several reports suggest that the treatment of nanoparticles caused the loss of cancer cells due to programmed cell death (Asiri et al., 2019; Khan, 2019; Khan, 2018).

The impact of AuNPs (Hibiscus) and AuNPs (Curcumin) on HCT-116 and MCF-7 was investigated using cell viability assay. The results of the cell viability assay are represented in Fig. 7. The results of this assay displayed a substantial decrease in the cell viability after the treatments of AuNPs -Hibiscus and AuNPs -Curcumin. However, AuNPs -Hibiscus is better in inhibiting the cancer cells than AuNPs -Curcumin as observed by Fig. 6b & e. It was observed that the inhibitory response on cancerous cells was dose-dependent in both AuNPs -Hibiscus and AuNPs -Curcumin specimens. We have also calculated the  $IC_{50}$  for both AuNPs -Hibiscus and AuNPs -Curcumin specimens as shown in the Table 1.

In addition, the impact of AuNPs -Hibiscus and AuNPs -Curcumin on non-cancerous cells, HEK-293 was also studied. The results did not show any significant inhibitory action on both non-cancerous cells and HEK-293 cells (see Fig. 8.) Several studies reported the successful inhibition of the cancer cells after treatments with different types of nanoparticles (Rehman, 2019; Khan, 2018; Akhtar et al., 2019). In addition, the extracts of Curcumin and hibiscus also caused anti-cancer activities in many studies (Hsu, 2015; Chen, 2020; Zhang, 2019; Hu, 2015; Laskar and Mazumder, 2020).

**Table 1** Impact of Au-NPs on HCT-116 and MCF-7 cells.

S. No.	NPs	HCT-116 ( $IC_{50}$ ) (µg/ml)	MCF-7 ( $IC_{50}$ ) (µg/ml)
1	AuNPs-Hibiscus	$5.80 \pm 0.91$ µg/ml	$3.62 \pm 0.75$ µg/ml
2	AuNPs-Curcumin	$4.94 \pm 0.85$ µg/ml	$3.91 \pm 0.65$ µg/ml

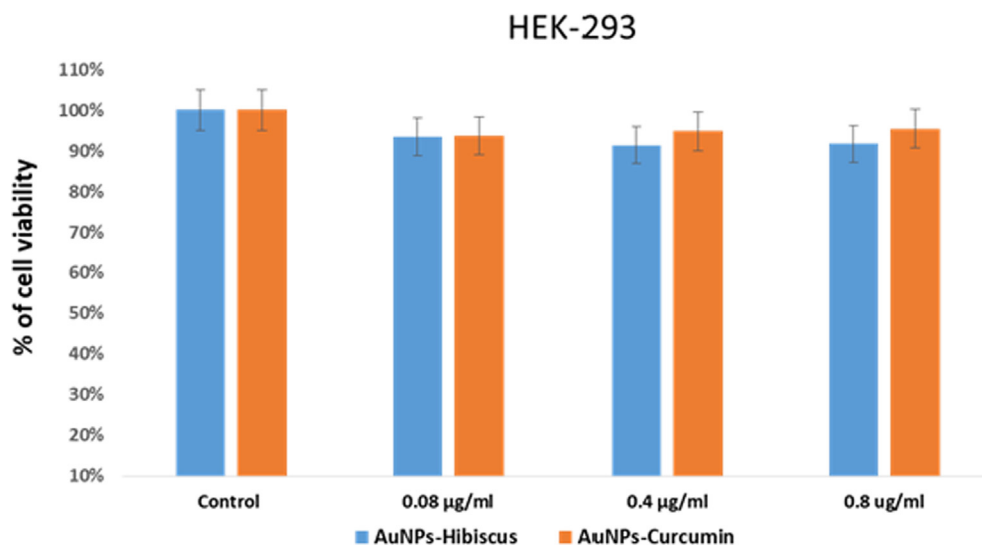


**Fig. 8** Cell viability assay: Impact of AuNPs-Hibiscus and AuNPs-Curcumin on human embryonic kidney cells (HEK-293).

#### 4. Conclusions

In this study, AuNPs were synthesized by employing an eco-friendly route, whereby Hibiscus and Curcumin extractions were used as reducing and stabilizing agents. The optical properties, chemical bonding and the morphology of the prepared AuNPs (AuNPs -Hibiscus and AuNPs -Curcumin) were characterized by UV-Vis spectroscopy, FTIR, SEM and TEM. The UV-Vis spectroscopy results confirmed the characteristics resonance peaks for gold. Electron microscopy (SEM and TEM) analyses revealed the spherical morphology of the particles with average size near to 20 nm. It was observed that the particles were well dispersed and perfect in shape when they were prepared under Hibiscus extraction. On the other hand, a slight aggregation or interconnected morphology was observed for AuNPs-Curcumin. The appearance of gold peaks in the EDS spectra confirmed the nature of AuNPs. The anti-cancer cell activity of the AuNPs was studied against HCT-116 and MCF-7 cells. It was observed that the treatment of cancer cells with AuNPs decreased the no. of cells significantly as compared to control cells. The AuNPs-Hibiscus specimen showed the better inhibiting properties than AuNPs-Curcumin, which is attributed to uniform dispersion and small size of the particles. No significant inhibitory action was noted on healthy cells (HEK-293 cells). The disintegration of cancer DNA study suggested that the decrease in the number of cancer cells were due to the cell death which was described by programmed cell death or apoptosis. The results of the cell viability assay showed a substantial decrease in the cell viability after treatment with both types of AuNPs.

#### Declaration of Competing Interest

The authors declare that they have no known competing financial interests or personal relationships that could have appeared to influence the work reported in this paper.

#### Acknowledgement

The authors acknowledge the Institute for Research and Medical Consultations (IRMC) at IAU, Saudi Arabia and RCSI Summer School, Medical University of Bahrain for providing the research facilities to complete this work. DR. S.A thanks to Mr. Edwardson to help for SEM and TEM sample preparation.

#### Appendix A. Supplementary data

Supplementary data to this article can be found online at <https://doi.org/10.1016/j.arabjc.2021.103594>.

#### References

- Lee, K.X. et al, 2020. Recent Developments in the Facile Bio-Synthesis of Gold Nanoparticles (AuNPs) and Their Biomedical Applications. *Int J Nanomedicine* 15, 275–300.
- Zhang, X., 2015. Gold Nanoparticles: Recent Advances in the Biomedical Applications. *Cell Biochem. Biophys.* 72 (3), 771–775.
- Xu, X.Y. et al, 2021. Biosynthetic gold nanoparticles of *Hibiscus syriacus* L. callus potentiates anti-inflammation efficacy via an autophagy-dependent mechanism. *Mater. Sci. Eng., C* 124, 112035.
- Taghizadeh, S. et al, 2019. Gold nanoparticles application in liver cancer. *Photodiagnosis Photodyn Ther* 25, 389–400.
- Vimalraj, S., Ashokkumar, T., Saravanan, S., 2018. Biogenic gold nanoparticles synthesis mediated by *Mangifera indica* seed aqueous extracts exhibits antibacterial, anticancer and anti-angiogenic properties. *Biomed. Pharmacother.* 105, 440–448.
- AbuMousa, R.A. et al, 2018. Photo-catalytic Killing of HeLa Cancer Cells Using Facile Synthesized Pure and Ag Loaded WO<sub>3</sub> Nanoparticles. *Sci. Rep.* 8 (1), 15224.
- Jermly, B.R. et al, 2021. PEGylated green halloysite/spinel ferrite nanocomposites for pH sensitive delivery of dexamethasone: A potential pulmonary drug delivery treatment option for COVID-19. *Appl. Clay Sci.* 9, (106333) 106333.
- Ansari, M.A. et al, 2021. Counteraction of Biofilm Formation and Antimicrobial Potential of Terminalia catappa Functionalized Silver Nanoparticles against *Candida albicans* and Multidrug-Resistant Gram-Negative and Gram-Positive Bacteria. *Antibiotics* 10 (6).
- Jain, S., Hirst, D.G., O'Sullivan, J.M., 2012. Gold nanoparticles as novel agents for cancer therapy. *British J. Radiology* 85 (1010), 101–113.
- Peng, J. and X. Liang, *Progress in research on gold nanoparticles in cancer management*. *Medicine*, 2019. 98(18): p. e15311-e15311.
- Elahi, N., Kamali, M., Baghersad, M.H., 2018. Recent biomedical applications of gold nanoparticles: A review. *Talanta* 184, 537–556.
- Yeh, Y.-C., Creran, B., Rotello, V.M., 2012. Gold nanoparticles: preparation, properties, and applications in bionanotechnology. *Nanoscale* 4 (6), 1871–1880.
- Daruich De Souza, C., Ribeiro Nogueira, B., Rostelato, M.E.C.M., 2019. Review of the methodologies used in the synthesis gold nanoparticles by chemical reduction. *J. Alloy. Compd.* 798, 714–740.
- Ahmed, S. et al, 2016. Biosynthesis of gold nanoparticles: A green approach. *J. Photochem. Photobiol., B* 161, 141–153.
- Zhao, P., Li, N., Astruc, D., 2013. State of the art in gold nanoparticle synthesis. *Coord. Chem. Rev.* 257 (3), 638–665.
- Kim, Y.H. et al, 2018. Antidepressant-Like and Neuroprotective Effects of Ethanol Extract from the Root Bark of *Hibiscus syriacus* L. *Biomed Res. Int.* 2018, 7383869.
- Yang, J.-E. et al, 2019. Dietary enzyme-treated *Hibiscus syriacus* L. protects skin against chronic UVB-induced photoaging via enhancement of skin hydration and collagen synthesis. *Arch. Biochem. Biophys.* 662, 190–200.
- Bindhu, M.R. et al, 2014. Antibacterial activities of *Hibiscus cannabinus* stem-assisted silver and gold nanoparticles. *Mater. Lett.* 131, 194–197.
- Hsu, R.J. et al, 2015. The triterpenoids of *Hibiscus syriacus* induce apoptosis and inhibit cell migration in breast cancer cells. *BMC Complement Altern Med* 15 (65), 015–0592.
- Al Shehab, S., Patra, D., 2021. Binding of metal ions to the curcumin mediated methoxy polyethylene glycol thiol conjugated green synthesized gold nanoparticles: A fluorescence spectroscopic study. *J. Photochem. Photobiol., A* 407, 113083.
- Muniyappan, N., Pandeewaran, M., Amalraj, A., 2021. Green synthesis of gold nanoparticles using *Curcuma pseudomontana* isolated curcumin: Its characterization, antimicrobial, antioxidant and anti-inflammatory activities. *Environ. Chem. Ecotoxicology* 3, 117–124.
- Wang, L. et al, 2019. Green synthesis of gold nanoparticles from *Scutellaria barbata* and its anticancer activity in pancreatic cancer cell (PANC-1). *Artif. Cells Nanomed. Biotechnol.* 47 (1), 1617–1627.
- Farooq, M.U. et al, 2018. Gold Nanoparticles-enabled Efficient Dual Delivery of Anticancer Therapeutics to HeLa Cells. *Sci. Rep.* 8 (1), 2907.
- Gu, X. et al, 2020. Preparation and antibacterial properties of gold nanoparticles: a review. *Environ. Chem. Lett.* 19, 167–187.

- Liu, S., Lämmerhofer, M., 2019. Functionalized gold nanoparticles for sample preparation: A review. *Electrophoresis* 40 (18–19), 2438–2461.
- Shahwan, T. et al, 2011. Green synthesis of iron nanoparticles and their application as a Fenton-like catalyst for the degradation of aqueous cationic and anionic dyes. *Chem. Eng. J.* 172 (1), 258–266.
- Akhtar, S. et al, 2020. Evaluation of bioactivities of zinc oxide, cadmium sulfide and cadmium sulfide loaded zinc oxide nanostructured materials prepared by nanosecond pulsed laser. *Mater. Sci. Eng., C* 116, 111156.
- Khan, F.A. et al, 2020. Quantum dots encapsulated with curcumin inhibit the growth of colon cancer, breast cancer and bacterial cells. *Nanomedicine* 15 (10), 969–980.
- Alheshibri, M. et al, 2021. Template-free single-step preparation of hollow CoO nanospheres using pulsed laser ablation in liquid environment. *Arabian J. Chem.* 14, (9) 103317.
- Akhtar, S. et al, 2018. Enhancement of anticorrosion property of 304 stainless steel using silane coatings. *Appl. Surf. Sci.* 440, 1286–1297.
- Mishra, P. et al, 2016. Facile bio-synthesis of gold nanoparticles by using extract of Hibiscus sabdariffa and evaluation of its cytotoxicity against U87 glioblastoma cells under hyperglycemic condition. *Biochem. Eng. J.* 105, 264–272.
- Sreelakshmi, C. et al, 2013. Green Synthesis of Curcumin Capped Gold Nanoparticles and Evaluation of Their Cytotoxicity. *Nanosci. Nanotechnol. Lett.* 5 (12), 1258–1265.
- Muniyappan, N., Nagarajan, N.S., 2014. Green synthesis of gold nanoparticles using Curcuma pseudomontana essential oil, its biological activity and cytotoxicity against human ductal breast carcinoma cells T47D. *J. Environ. Chem. Eng.* 2 (4), 2037–2044.
- Sun, Y., Xia, Y., 2003. Gold and silver nanoparticles: A class of chromophores with colors tunable in the range from 400 to 750 nm. *Analyst* 128 (6), 686–691.
- Slocik, J.M. et al, 2008. Colorimetric response of peptide-functionalized gold nanoparticles to metal ions. *Small* 4 (5), 548–551.
- Ismail, E.H. et al, 2018. Successful Green Synthesis of Gold Nanoparticles using a Corchorus olitorius Extract and Their Antiproliferative Effect in Cancer Cells. *Int. J. Mol. Sci.* 19 (9).
- Bhuyan, B., et al., Paederia foetida Linn. promoted biogenic gold and silver nanoparticles: Synthesis, characterization, photocatalytic and in vitro efficacy against clinically isolated pathogens. *J Photochem Photobiol B*, 2017. 173: p. 210-215.
- Philip, D., 2010. Green synthesis of gold and silver nanoparticles using Hibiscus rosa sinensis. *Physica E* 42 (5), 1417–1424.
- Gurunathan, S. et al, 2014. A green chemistry approach for synthesizing biocompatible gold nanoparticles. *Nanoscale Res. Lett.* 9 (1), 9–248.
- Ankamwar, B., Chaudhary, M., Sastry, M., 2005. Gold Nanotriangles Biologically Synthesized using Tamarind Leaf Extract and Potential Application in Vapor Sensing. *Synth. React. Inorg., Met.-Org., Nano-Met. Chem.* 35 (1), 19–26.
- Sneha, K. et al, 2010. Counter ions and temperature incorporated tailoring of biogenic gold nanoparticles. *Process Biochem.* 45 (9), 1450–1458.
- Krishnamurthy, S. et al, 2014. Yucca-derived synthesis of gold nanomaterial and their catalytic potential. *Nanoscale Res. Lett.* 9 (1), 627.
- Asiri, S.M., Khan, F.A., Bozkurt, A., 2019. Delivery of Conjugated Silicon Dioxide Nanoparticles Show Strong Anti-Proliferative Activities. *Appl. Biochem. Biotechnol.* 189 (3), 760–773.
- Khan, F.A. et al, 2019. Targeted delivery of poly (methyl methacrylate) particles in colon cancer cells selectively attenuates cancer cell proliferation. *Artif. Cells Nanomed. Biotechnol.* 47 (1), 1533–1542.
- Khan, F.A. et al, 2018. Fluorescent magnetic submicronic polymer (FMSP) nanoparticles induce cell death in human colorectal carcinoma cells. *Artif. Cells Nanomed. Biotechnol.*, 1–7
- Rehman, S. et al, 2019. Biocompatible Tin Oxide Nanoparticles: Synthesis, Antibacterial, Anticandidal and Cytotoxic Activities, *ChemistrySelect*.
- Khan, F.A. et al, 2018. Extracts of Clove (Syzygium aromaticum) Potentiate FMSP-Nanoparticles Induced Cell Death in MCF-7 Cells. *Int. J. Biomaterials*.
- Akhtar, S., Khan, F.A., Buhaimeed, A., 2019. Functionalized magnetic nanoparticles attenuate cancer cells proliferation: Transmission electron microscopy analysis. *Microsc. Res. Tech.* 82 (7), 983–992.
- Chen, Y. et al, 2020. Nano Encapsulated Curcumin: And Its Potential for Biomedical Applications. *Int. J. Nanomed.* 15, 3099–3120.
- Zhang, Y. et al, 2019. Advances in curcumin-loaded nanopreparations: improving bioavailability and overcoming inherent drawbacks. *J. Drug Target.* 27 (9), 917–931.
- Hu, B. et al, 2015. A polymeric nanoparticle formulation of curcumin in combination with sorafenib synergistically inhibits tumor growth and metastasis in an orthotopic model of human hepatocellular carcinoma. *Biochem. Biophys. Res. Commun.* 468 (4), 525–532.
- Laskar, Y.B., Mazumder, P.B., 2020. Insight into the molecular evidence supporting the remarkable chemotherapeutic potential of Hibiscus sabdariffa L. *Biomed. Pharmacother.* 127 (110153), 27.